ECS Transactions, 35 (1) 727-737 (2011)
10.1149/1.3570052 ©The Electrochemical Society

Combined Theoretical and Experimental Studies of H_2 and CO Oxidation over YSZ Surface

Alexandr Gorski[a], Vitaliy Yurkiv[a,b], Wolfgang G. Bessler[b], Hans-Robert Volpp[a]

[a] Institute of Physical Chemistry, Heidelberg University, 69120 Heidelberg, Germany
[b] German Aerospace Center (DLR), Institute of Technical Thermodynamics
70569 Stuttgart, Germany

The mechanism of H_2 and CO adsorption and oxidation on yttria-stabilized zirconia, frequently used as electrolyte in solid oxide fuel cell composite anodes, was investigated employing temperature-programmed spectroscopy (TPS) and density functional theory (DFT). In agreement with theory, the experimental results show that interaction of gaseous H_2O with YSZ results in dissociative adsorption leading to strongly bound OH surface species. In the interaction of gaseous H_2 with an oxygen-enriched YSZ surface (YSZ+O), similar OH surface species are formed as reaction intermediates in the H_2 oxidation. In contrast, the interaction of CO with an oxygen-enriched YSZ leads to direct formation of gaseous CO_2 via an Eley-Rideal type reaction that was also confirmed by TPS measurements.

Introduction

In practical solid oxide fuel cell (SOFC) systems, nickel and yttria-stabilized zirconia (Ni/YSZ) composites are frequently used as anodes. The elucidation of the microscopic details of the electrochemical reaction mechanism requires elementary kinetic numerical simulations along with electrochemical characterization experiments performed with geometrically well-defined model anode structures (1, 2).

The important attribute of SOFC is the ability to operate with a variety of fuels, that is, CO/H_2 and hydrocarbons (2, 3). However, because of many difficulties in use of latter fuels (deposit formation associated with pure hydrocarbon fuels, anode oxidation etc.) the simplest system, namely $H_2/H_2O/Ni/YSZ$ and $CO/CO_2/Ni/YSZ$, should be investigated, in order to understand the elementary processes taking place at the triple phase boundary (TPB), between a Ni anode, a YSZ electrolyte and a gas phase. In this case, adsorption/desorption/diffusion and thermally activated surface reactions provide the boundary conditions for the actual charge transfer reactions which take place at the TPB and which are almost impossible to study directly on a microscopic level. Therefore, many modern computational approaches have been aimed on the elucidation and quantification of the charge transfer processes. The availability of reliable electroneutral thermal surface adsorption/desorption and surface reaction is mandatory in the light of the complex interaction between thermal and electrochemical surface reactions. With no reliable thermal reaction data sets the model-based analysis is not more than a multi-parameter fitting with the results that provide no clear physical information.

The importance of chemical reactions at the YSZ surface under SOFC operation was shown by several groups (1, 4-6). However, despite the work that has been done, the detailed kinetics of the fuels (e.g., H_2 and CO) interaction with YSZ surface is not well understood. The present work is focused on elementary kinetics of H_2 and CO adsorption/desorption and oxidation on YSZ surface. In addition, the discussion of CO oxidation on Ni surface is included. The investigation of CO oxidation is appealing because it is a major component of reformate gases and is formed in situ when using hydrocarbons, both of which are relevant fuels in technical SOFC systems (1, 2, 7). At the same time, reformate gases contain a substantial amount of H_2 and H_2O. In such a mixture, it is still unclear whether CO oxidation proceeds directly (Langmuir-Hinshelwood (LH) or Eley-Rideal (ER) type mechanisms) or indirectly (water-gas shift reaction). In order to elucidate the mechanism and pathways of reformate gases oxidation, it is important to analyze the intrinsic reaction kinetics of H_2 and CO oxidation on YSZ and Ni surfaces alone.

Various H_2/H_2O/Ni/YSZ and CO/CO_2/Ni/YSZ electrode kinetics models have been employed recently (1, 4, 5, 8). As outlined in (1), the available electrode kinetics models mainly disagree with regard to the actual location – either mainly on the Ni or both on the Ni and on the YSZ surfaces – where the heterogeneous chemical and electrochemical elementary reaction steps take place. Sensitivity analyses performed in the course of the recent studies (1, 4) clearly emphasize the great influence of the thermodynamic and reaction kinetics data of YSZ surface species on the electrochemical modeling results (see e.g., Fig. 11 of Ref. (1) and Fig. 5 of Ref. (4)). In addition, the formation of interstitial hydrogen and hydroxyl at the Ni electrode/YSZ electrolyte two-phase boundary was proposed in Ref. (9) and confirmed by Gorski et al. (10).

Experimental and Theoretical Methodology

Temperature-Programmed Desorption and Reaction

Temperature-programmed desorption (TPD) and temperature-programmed reaction (TPR) experiments of H_2 and CO adsorption/desorption and oxidation on the YSZ surface were performed under molecular flow conditions in a reaction chamber, which has been described elsewhere (8). In the present work polycrystalline YSZ samples (8.5% mol Y_2O_3) with a thickness of 0.2 mm were employed. The original YSZ sample plate was obtained from Itochu (Tokyo, Japan). As stated by the manufacturer, only trace amounts of impurities, such as Al and Si, are present in the samples. In order to estimate the amount of impurities, the X-ray photoelectron spectroscopy (XPS) measurements were performed. Based on XPS measurements (not shown here), only Si was detected in YSZ sample with a concentration of about 1 %. Aluminum was not detected. In the TPD/TPR measurements, the temperature of the YSZ samples could be varied from 300 K up to 1200 K. The substrate temperature was measured by a thermocouple attached to the sample surface.

The simulations of TPD/TPR experimental spectra were carried out using the software package DETCHEM (11), which allows the calculation of temperature- and time-dependent surface coverages and surface species fluxes in the framework of a zero-

dimensional surface reaction model employing thermodynamically consistent reversible elementary reaction kinetics.

Quantum Chemical Calculations

Quantum chemical calculations based on density functional theory (DFT) were performed to investigate H_2 and CO adsorption/desorption and oxidation energetics on the YSZ surface. As in our previous DFT study (10, 12) the present calculations were performed using the CASTEP (Cambridge Sequential Total Energy Package) computer code (13) in the framework of the generalized gradient approximation (GGA), as proposed by Perdew and Wang (14), in combination with Vanderbilt ultrasoft pseudopotentials (15). For systems with an even number of electrons restricted nonspin-polarized calculations were performed. For systems with an odd number of electrons unrestricted spin-polarized calculations were performed. The plane wave basis set was truncated at a kinetic energy of 420 eV. Computations were performed over a range of k-points within the Brillouin zone as generated by the full Monkhorst-Pack scheme (16) with a 2×2×1 mesh. A further increase of the cut off energy and the number of *k*-points resulted in negligibly small changes in adsorption energies (typically less than 5 kJ mol^{-1}), indicating that the energy values are well converged. A slab was repeated periodically, leaving at least a 10 Å wide vacuum region in the direction perpendicular to the surface. The atoms of the bottom multilayer were fixed in all calculations, while the positions of atoms of the two outermost multilayers and the positions of atoms of the adsorbed molecules were optimized during the process of structural relaxation. A complete linear synchronous transit (LST)/quadratic synchronous transit (QST) scheme (17) was used in the transition state searches for the surface reaction steps. A force convergence criterion of 0.03 eV·$Å^{-1}$ was applied in all calculations.

The slabs used in the present study to investigate H_2 oxidation on an oxygen-enriched YSZ surface, denoted as YSZ+O in the following, and H_2O dissociation on a YSZ surface are reproduced in Figs. 1a and 1b, respectively. The procedure applied to obtain a representative slab for the (111) surface of YSZ as shown in Fig. 1b is similar to the one described in Ref. (5), which starts from a pure (111) terminated zirconia slab, which consists of 12 ZrO_2 formula units with 36 atoms (for further details see Ref. (5) and Fig. 2 therein). From the pure zirconia slab an oxygen atom was removed to account for vacancy formation (denoted as "vac." in Fig. 1b) and two zirconium atoms were substituted by two yttrium atoms which are depicted as green atoms (Y) corresponding to a 9% mol concentration of yttria in YSZ. Finally, in order to generate an oxygen-enriched surface, an additional oxygen atom (marked by $*$ in Fig. 1a) was introduced to occupy the subsurface oxygen vacancy of YSZ. The four different surface oxygen atoms of the YSZ+O surface unit cell are indicated by the numbering (i = 1-4). The obtaining of oxygen-enriched YSZ surface (YSZ+O) under practical conditions is certainly depends on the actual SOFC fuel gas operating and polarization conditions in the anode polarization measurement. An anodic polarization (oxygen being pumped to the anode) certainly helps to maintain the oxygen-rich YSZ-O, while cathodic polarization conditions (oxygen being pumped away from the anode) favor the presence of reduced oxygen-poor YSZ. The inclusion of such a mechanism capable to describe the polarization dependent (surface oxygen dependent) modification of reactivity of the electrolyte surface in the vicinity of the TPB, as suggested by our DFT results, is

certainly desirable in order to investigate the influence on the electrochemical modeling results.

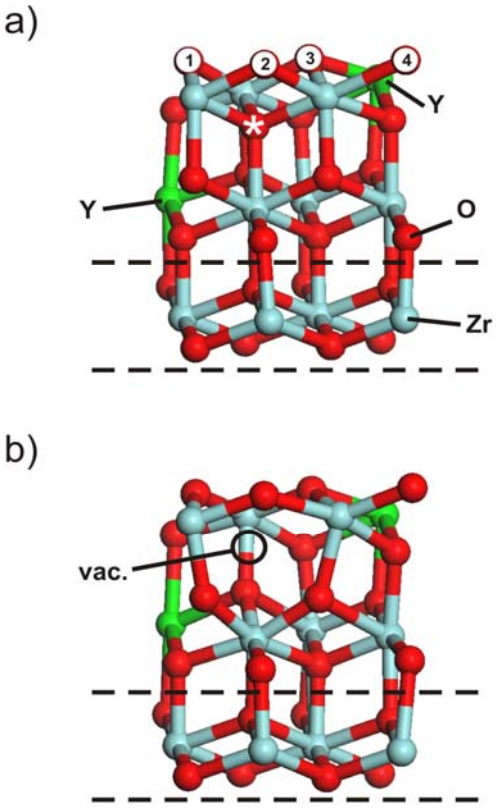

Figure 1. Slabs employed in the present DFT calculations: (a) Oxygen rich YSZ+O with the additional oxygen atom (∗) occupying the subsurface oxygen vacancy of YSZ, the structure of which is reproduced in (b) with the positing of the subsurface oxygen vacancy marked as "vac." For further details see text.

Results and Discussion

Quantum Chemical Calculations

H_2 Oxidation on YSZ. In Fig. 2 the low energy reaction pathway for the heterogeneous H_2 oxidation reaction on the YSZ+O surface as obtained in the DFT calculations is schematically depicted. The pathway shown in Fig. 2 leads to direct formation of gaseous $H_2O_{(g)}$ and YSZ by barrier less dissociative adsorption of H_2 on surface oxygen atoms via the formation of OH surface intermediates, which can further react to yield surface H_2O that finally desorbs into the gas phase leaving back a YSZ surface. The energetics of the reaction pathway corresponding to Fig. 2 is depicted in Fig. 3. The latter results also reveal that the reverse reaction, namely the dissociative adsorption of H_2O on YSZ leading to surface OH, is an activated process with overall DFT activation energies of E_a = 74.1 kJ mol^{-1}. The latter pathway involved the O4 surface atom of YSZ+O, Fig. 2. This pathway appears the most energetically stable from all recently tested pathways (9).

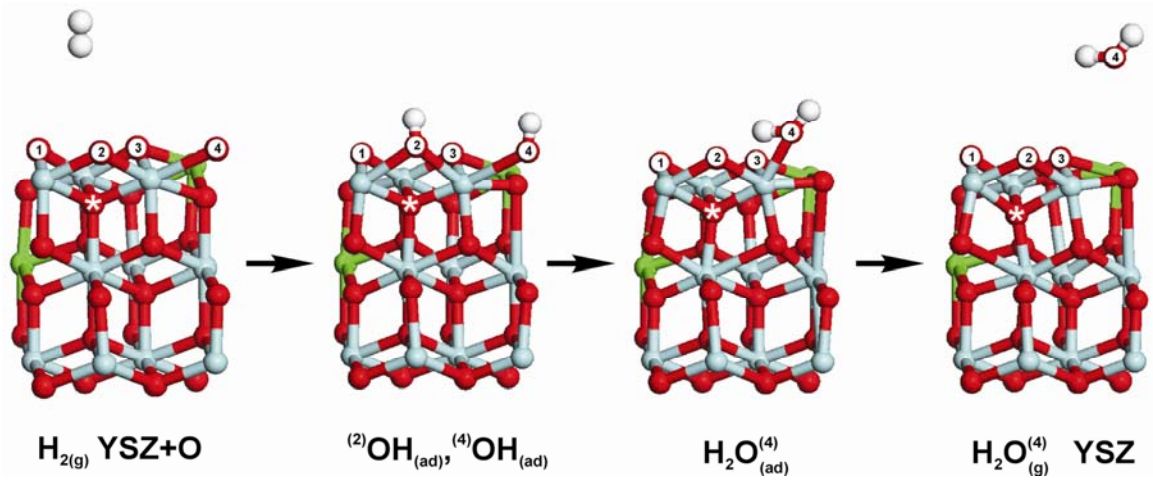

Figure 2. Illustration of surface reaction pathway as obtained in the present DFT studies of heterogeneous H_2 oxidation on YSZ+O surface.

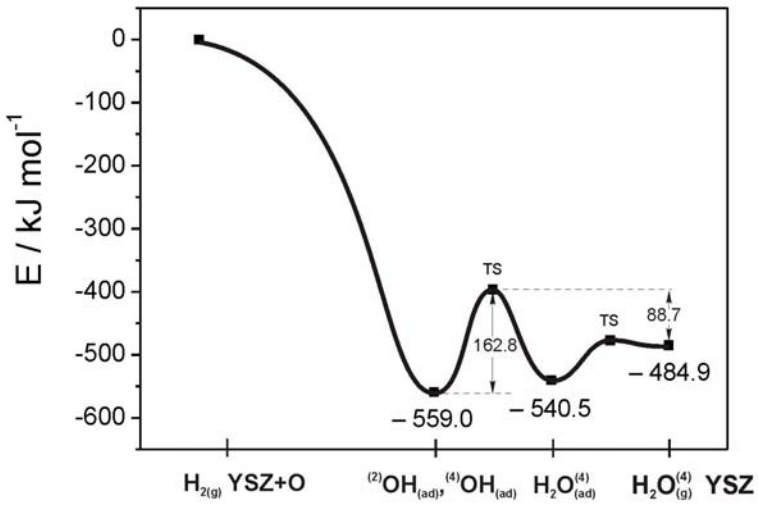

Figure 3. Energetic pathways for the surface reactions illustrated in Fig. 2.

CO Oxidation on YSZ. We have investigated the oxidation of the CO molecule over the YSZ and YSZ+O surfaces. On the YSZ+O surface, the CO molecule can get oxidized by taking one of the four surface oxygen atoms (see Fig. 1a)). The mechanism of CO oxidation is described as

$$CO + O_{YSZ} \rightleftharpoons CO_2 + \square_{YSZ}. \qquad [1]$$

As was obtained in the investigation of H_2 oxidation (see Fig. 2 and Fig. 3), the lowest energy pathway, which leads to direct formation of gaseous H_2O, was found for the oxygen atom denoted as O4. The same scenario was observed for CO oxidation on YSZ+O surface, where CO is oxidized on O4 oxygen atom with the most favorable energetics. The latter process is shown in Fig. 4. The calculations revealed that the adsorption of a CO molecule lead to immediate formation of carbon dioxide (CO_2). It means that CO oxidation is occurred by an Eley-Rideal type reaction, where only one adsorbed species (oxygen on YSZ surface) is involved.

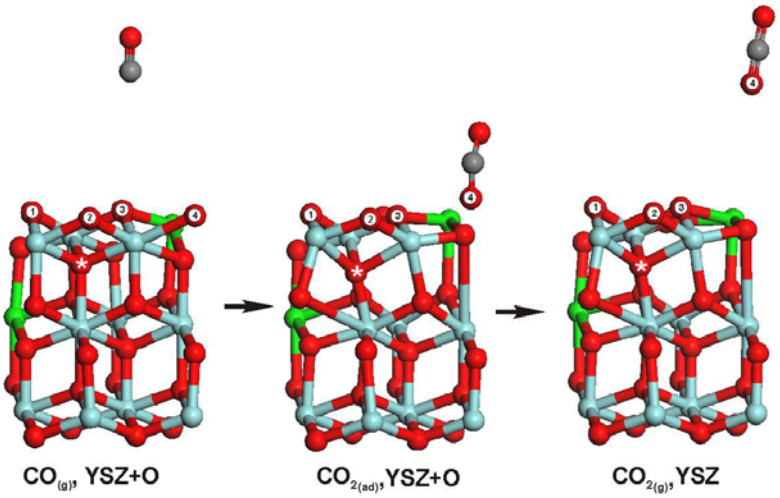

Figure 4. Illustration of surface reaction pathway as obtained in the present DFT studies for heterogeneous CO oxidation on the YSZ+O surface.

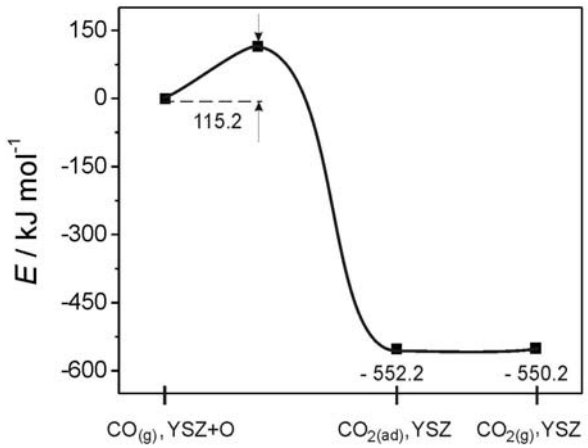

Figure 5: The energetics of the CO oxidation reaction on O4 oxygen atom as shown in Fig. 4.

The energetics of the reaction pathway of CO oxidation is illustrated in Fig. 5. The formation of CO_2 occurs with an activation energy of 115.3 kJ mol^{-1} and a decrease in enthalpy by –552.2 kJ mol^{-1}. The formed CO_2 molecule is weakly adsorbed via its oxygen atom. Desorption of the CO_2 molecule into the gas phase is accompanied by a small increase of enthalpy by 2 kJ mol^{-1} (–550.2 kJ mol^{-1}). Also, there is no barrier for the backward reaction of carbon dioxide adsorption on the YSZ surface.

Our findings indicate that CO oxidation on a YSZ+O surface is a highly exothermic process which occurs with significant activation energy. Desorption of the CO_2 molecule into gas phase does not take place with an activation barrier but only with a slight increase in enthalpy. The obtained results of CO oxidation over YSZ+O surface is in reasonable agreement with the one reported by Shishkin et al. (5). They showed that CO oxidation on the YSZ+O surface is very favorable with substantial energy decrease by –489.1 kJ mol^{-1}. However, Shishkin et al. did not comment on activation barrier of CO_2 formation as well as CO_2 dissociation.

In contrast to YSZ+O, the oxidation of CO on YSZ surface, where one oxygen atom is removed (Fig. 1b)) was not observed. Only physisorption of carbon monoxide was identified on YSZ surface. On the oxygen atoms within YSZ surface, the adsorption of carbon monoxide is an endothermic process with the enthalpy of +9.7 kJ mol^{-1} (O1 and O2 oxygen atoms), +26.7 kJ mol^{-1} (O3 oxygen atom) and +17.4 kJ mol^{-1} (O4 oxygen atom). Also, the possibility of CO adsorption on metals (Y, Zr) was investigated. Here, CO adsorbs exothermically with decrease in enthalpy by –32.6 kJ mol^{-1} when the molecule is bonded to an yttrium atom and by –20 kJ mol^{-1} when adsorbed on zirconium atom.

Experimental Studies of Heterogeneous Chemistry of H_2/H_2O and CO/CO_2 on YSZ

H_2O on YSZ. A series of TPD/TPR measurements was performed for the YSZ sample, where the sample was exposed to different gas compositions and described in details in Ref. (9). Fig. 6 shows the comparison between theoretical and experimental TPR spectra, where the YSZ sample was exposed to a H_2/O_2 mixture ($p(H_2) = p(O_2) = 1 \cdot 10^{-6}$ mbar) for 25 minutes prior to TPD spectra measurements. The adsorption/desorption and surface reaction kinetics data set was obtained in the present work by systematically adjusting the respective pre-exponential factor values (k^0) in the TPD simulation until best agreement with the experimental TPD spectra was achieved. The values for the respective Arrhenius activation energies (E_a) were taken from the DFT calculation results represented in Fig. 3. The comparison between simulated and experimentally measured H_2O TPD spectra where the YSZ sample was exposed to ambient air humidity also leads to good agreement (Fig. 7).

CO on YSZ. CO oxidation was studied on the YSZ surface for a CO partial pressure of $p(CO) = 10^{-6}$ mbar and an O_2 partial pressure of $p(O_2) = 10^{-6}$ mbar. Experimental spectra were recorded with a heating rate of 5 $K \cdot s^{-1}$. Experimental results are shown in Fig. 8 together with the results of the numerical simulation. The experimental and theoretical observations show that the CO_2 formation starts at a temperature of ca. 600 K, where no CO is present on the YSZ surface. The latter fact, along with the observation of a substantial decrease of the CO gas-phase pressure at ca. 725 K (which closely follows the CO_2 formation data curve), indicates that CO oxidation over YSZ proceeds predominately via an ER reaction mechanism. In this mechanism, gas-phase CO directly reacts with YSZ oxygen surface atoms, O_{YSZ}, to yield gas-phase CO_2. By fitting the numerical simulations to the experiment, using value for activation energy of 115.2 kJ/mol from present DFT calculation (Fig. 5), a pre-exponential factor of $1.0 \cdot 10^{23}$ cm^2 $(mol\ s)^{-1}$ was derived for the $CO + O_{YSZ} \rightarrow CO_2 + \square_{YSZ}$ surface reaction step.

CO Oxidation on Ni Surfaces

We also performed comprehensive DFT calculations to investigate the CO oxidation on the Ni surface, due to its importance as the step of fuel oxidation in SOFC operations. For these types of calculations we used the same code as in DFT calculation on YSZ surface. However, an different nonlocal functional, RPBE (18), a revised form of the PBE functional designed by Hammer et al., to improve the description of metallic surfaces, was used to investigated the CO adsorption/desorption energies and oxidation mechanism on Ni(111) surface. The plane wave basis set was truncated at a kinetic energy of 380 eV. In the case of Ni surface, the range of k-points was changed to 3x3x1

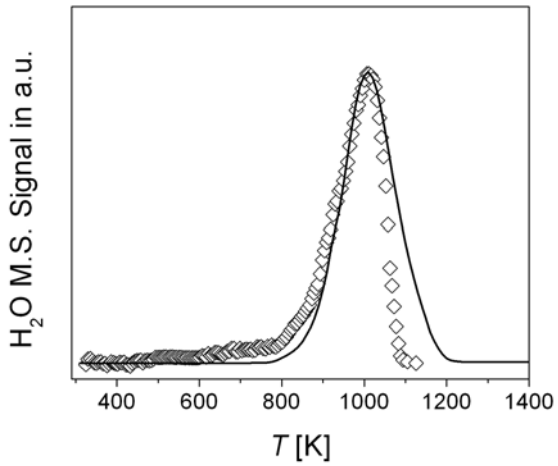

Figure 6. Comparison between simulated (solid line) and experimental (open symbols) TPD spectrum of H_2O desorption from YSZ surface. The heating rate is 1 $K \cdot s^{-1}$, the pressures of H_2 is $p(H_2) = 10^{-6}$ mbar and O_2 - $p(O_2) = 10^{-6}$ mbar.

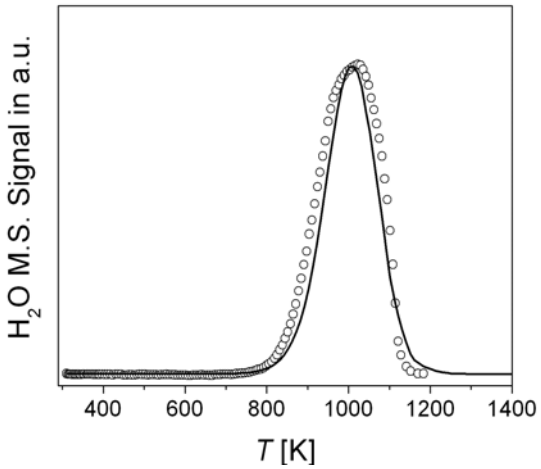

Figure 7. Comparison between simulated (solid line) and experimental (open symbols) TPD spectrum of H_2O desorption from YSZ surface. The heating rate is 1 $K \cdot s^{-1}$, the sample was exposed to ambient air humidity.

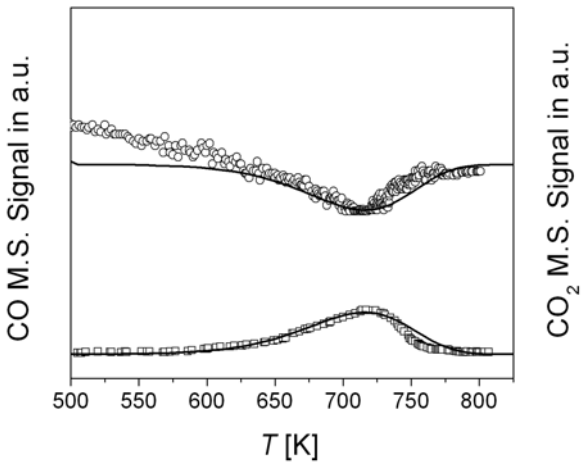

Figure 8. Comparison between simulated (solid lines) and experimental (open symbols) TPD and TPR spectra of CO and CO_2 on YSZ. The heating rate is 1 $K \cdot s^{-1}$, the pressures of CO is $p(CO) = 10^{-6}$ mbar and O_2 - $p(O_2) = 10^{-6}$ mbar.

mesh. The Ni surface was modeled as a 2x2 Ni atoms slab with the thickness of 5 atomic layers. A 15 Å vacuum slab has been used for surface relaxation and reaction transition state search. The positions of the metal atoms were fixed in (111) surface configuration, while the positions of the CO surface adsorbates were fully mobile.

As in the case of YSZ surface, for this reaction system we also obtained an ER type reaction during the CO oxidation on Ni(111) surface. The reaction pathway of CO oxidation, as obtained in the present DFT calculations, is depicted in Fig. 9, and the energetics are shown in Fig. 10. The present results indicate that the overall reaction $CO_{(g)} + O_{Ni} \rightarrow CO_{2(g)} + \square_{Ni}$ is exothermic with the enthalpy decrease by 79.1 kJ mol^{-1}. Furthermore, as shown in Fig. 10, the CO oxidation is accompanied by activation energy of 181.8 kJ mol^{-1}, which is expected while oxygen is strongly adsorbed to the Ni surface.

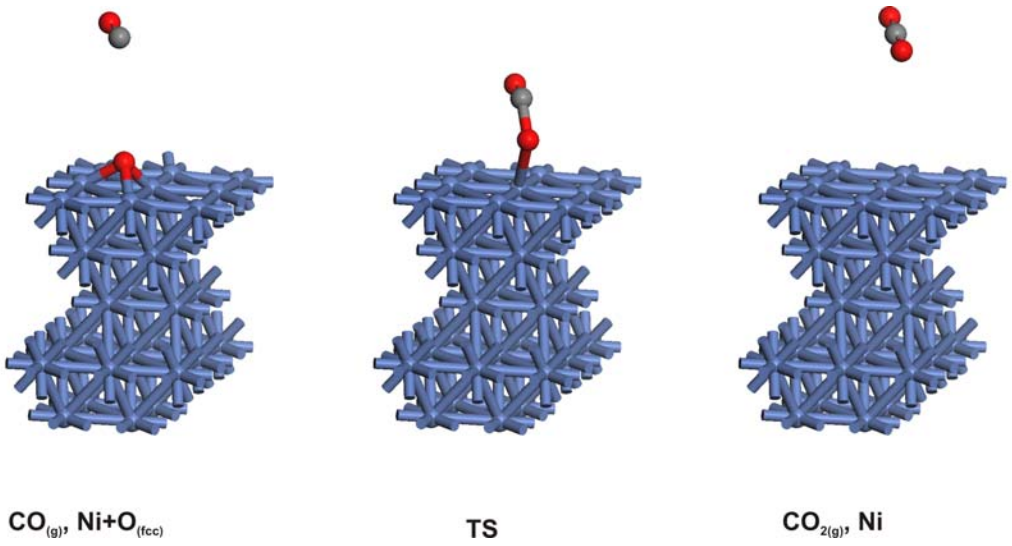

Figure 9. Illustration of surface reaction pathway as obtained in the DFT studies of heterogeneous CO oxidation on Ni(111) surfaces.

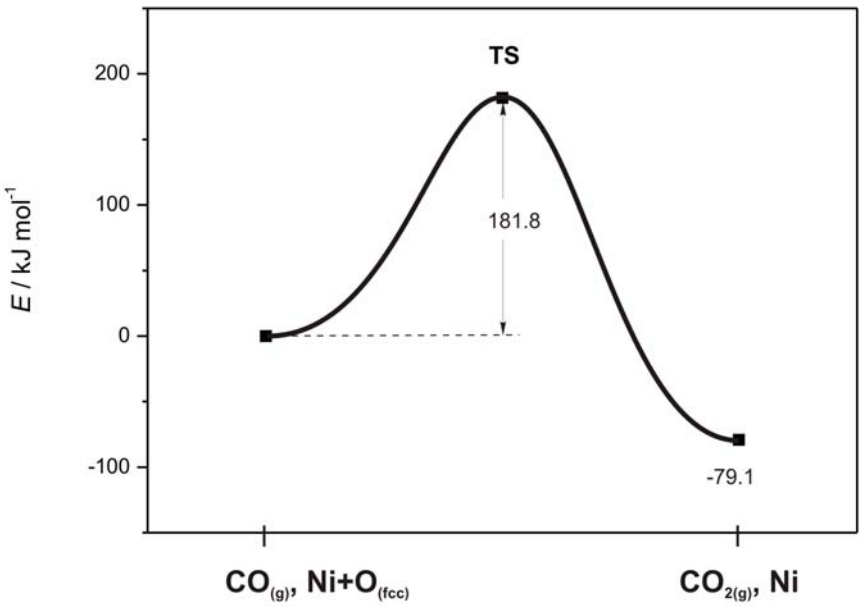

Figure 10: The energetics of the CO oxidation reaction on Ni(111) as shown in Fig. 9.

In light of the latter results, we believe that an ER-type CO oxidation mechanism on the Ni surface may strongly contribute to the SOFC electrochemical kinetics. In addition, we would like to note that the theoretically proven possibility for an ER-type CO oxidation reaction on Ni, along with the derived kinetics parameters, is a new finding. This reaction might also play a role if a more complex fuel such as reformate gas is used.

Conclusions

The present DFT results, along with TPD/TPR experiments, of CO and H_2 interaction with YSZ and YSZ+O model surfaces demonstrate the important role of the chemical state of the electrolyte surface (oxygen poor versus oxygen rich). In agreement with previous DFT studies (6. 10), the present results emphasize the influence of the additional oxygen atom – supplied either by dissociative adsorption of gaseous O_2 or via bulk oxygen atoms – on the surface reactivity. Under conditions where external oxygen supply maintains the surface in an oxygen rich (YSZ+O) state, fuels can easily get oxidized. In the case of CO oxidation, this leads to direct CO_2 formation via ER reaction type, and in the case of H_2, the surface gets hydroxylated with the direct formation of H_2O. Under surface oxygen depleting operating conditions, the resulting YSZ surface is virtually inert toward CO and H_2 oxidation. Hence, it seems not unreasonable to anticipate that the electrode polarization (anodic versus cathodic) could have a pronounced influence on the actual surface reactivity of the electrolyte.

Acknowledgments

The authors thank the German Research Foundation (DFG) for financial support of the experimental work under grants number VO 642/2-1 and BE 3819/1-1. V. Yurkiv and A. Gorski would like to thank the International Graduate College (IGK 710) “Complex Processes: Modeling, Simulation and Optimization” at the University of Heidelberg for fellowships.

References

1. W. G. Bessler, M. Vogler, H. Störmer, D. Gerthsen, A. Utz, A. Weber, E. Ivers-Tiffee , *Phys. Chem. Chem. Phys.*, **12**(42), 13888 (2010).
2. S. C. Singhal, K. Kendall, *High-temperature Solid Oxide Fuel Cells: Fundamentals, Design and Applications*, Elsevier Science, Oxford (2003).
3. S. B. Adler, W. G. Bessler, *Handbook of Fuel Cells*, *Advances in Electrocatalysis, Materials*, **5**(29), 441 (2010).
4. M. Vogler, A. Bieberle-Hütter, L. J. Gauckler, J. Warnatz, W. G. Bessler, , *J. Electrochem. Soc.*, **156**(5), B663 (2009)
5. D. G. Goodwin, H. Zhu, A. M. Colclasure, R. J. Kee, *J. Electrochem. Soc.*, **156**(9), B1004 (2009).
6. M. Shishkin, T. Ziegler, *Journal of Physical Chemistry C*, **112**(49), 19662 (2008).
7. V. M. Janardhanan, O. Deutschmann, *J. Power Sources*, **162**, 1192 (2006).
8. V. Yurkiv, D. Starukhin, H.-R. Volpp, W. G. Bessler, *J. Electrochem. Soc.*, **158**(1), B5 (2011).

9. M. Vogler, W. G. Bessler, *ECS Trans.*, **25**(2), 1957 (2009).
10. A. Gorski, V. Yurkiv, D. Starukhin, H.-R. Volpp, *J. Power Sources*, doi:10.1016/j.jpowsour.2010.09.090 (2010).
11. O. Deutschmann, S. Tischer, S. Kleditzsch, V. M. Janardhanan, C. Correa, D. Chatterjee, N. Mladenov, H. D. Mihn, *DETCHEM Software package, 2.1 ed., www.detchem.com.* (2007).
12. O. R. Inderwildi, D. Starukhin, H.-R. Volpp, D. Lebiedz, J. Warnatz, in *Quantum Chemical Calculations of Surfaces and Interfaces of Materials*, American Scientific Publishers (2009).
13. M. D. Segall, P. J. D. Lindan, M. J. Probert, C. J. Pickard, P. J. Hasnip, S. J. Clark, M. C. Payne, *J. Phys-Condens. Mat.*, **14**, 2717 (2002).
14. J. P. Perdew, J. A. Chevary, S. H. Vosko, K. A. Jackson, M. R. Pederson, D. J. Singh, C. Fiolhais, *Phys. Rev. B*, **46**, 6671 (1992).
15. D. Vanderbilt, *Phys. Rev. B*, **41**, 7892 (1990).
16. H. J. Monkhorst, P. J. Pack, *Phys. Rev. B*, **13**, 5188 (1976).
17. N. Govind, M. Petersen, G. Fitzgerald, D. King-Smith, J. Andzelm, *Comp. Mater. Sci*., **28**, 250 (2003).
18. B. Hammer, L. B. Hansen, J. K. Norskov, *Phys. Rev. B*, **59**, 7413 (1999).